

Light-Activated Hypoxia-Responsive Nanoparticles for Photodynamic Chemotherapy

Dan Zhao, Shunliang Zheng, Xinyi Zuo, Hongyang Xu,* Yue Ding,* and Fengming Liang*

Cite This: *ACS Omega* 2025, 10, 22719–22724

Read Online

ACCESS |



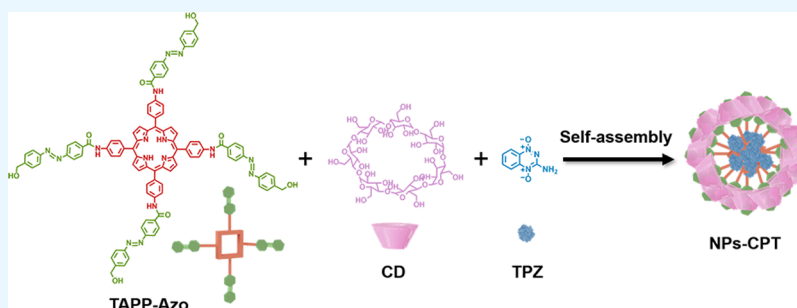
Metrics & More



Article Recommendations



Supporting Information



ABSTRACT: Hypoxia is a characteristic of solid tumors, and it significantly impedes cancer treatment. Here, we report light-activated hypoxia-responsive nanoparticles NPs-TPZ consisting of 5,10,5,20-tetrakis(4-aminophenyl)-porphine (TAPP) modified with four azobenzene groups, cyclodextrin (CD), and 3-aminobenzotriazine-1,4-di-N-oxide tirapazamine (TPZ) by the synergy of π - π stacking, host-guest, and hydrophobic interactions for synergistic photodynamic chemotherapy (PDT-CT). Under near-infrared (NIR) irradiation, the process of PDT depletes oxygen and generates singlet oxygen ($^1\text{O}_2$). The induced hypoxia exacerbation further accelerates the release and activation of TPZ. As a result, this hypoxia-responsive nanoparticle provides an effective strategy for the ablation of hypoxic solid tumors by synergistic PDT-CT.

1. INTRODUCTION

Photodynamic therapy (PDT), a clinically approved therapeutic approach that employs reactive oxygen species (ROS) produced by photosensitizers under light exposure to harm malignant cells, has been profoundly investigated in recent years.^{1–4} It possesses the benefits of extremely low toxicity to tissue, nearly no systemic adverse effects, no drug-induced immunosuppression, and high spatiotemporal precision.^{5,6} However, the restricted water solubility and tumor selectivity of the majority of photosensitizers have an impact on the efficacy of PDT and might cause phototoxicity to the adjacent normal tissues.⁷ To further boost the potency of PDT, the water-soluble macrocyclic molecules featuring a cavity are widely employed to construct host-guest complexation through loading the photosensitizer guest based on host-guest interactions.^{8,9} The major macrocyclic hosts encompass calixarenes, cyclodextrins, and pillararenes.^{10–13} In addition, photosensitizer-mediated PDT still presented considerable challenges despite its considerable potential. In fact, the oxygen consumption during photochemical reactions exacerbated the degree of hypoxia in the surrounding tumor microenvironment, hampering the therapeutic effect.¹⁴

To address these issues, various therapeutic methods such as oxygen codelivery and hyperthermia were employed to alleviate the hypoxic microenvironment.^{15,16} However, because of the complexity and variability of cancer, tumor cells survive

by other means. Rather than focusing on overcoming hypoxia, it seems to make more sense to use it through “hypoxia activation treatment strategies”.^{17–22} One of the effective strategies is developing hypoxia-activated prodrugs, such as 3-aminobenzotriazine-1,4-di-N-oxide tirapazamine (TPZ) and banoxantrone dihydrochloride (AQ4N).^{23–26} TPZ is an intermediate cytotoxic form that produces free radicals through cell reductase metabolism and is readily oxidized back to inactive prodrugs under normoxic conditions. Nevertheless, the highly reactive TPZ radicals are able to initiate radical-mediated DNA cleavage and eliminate hypoxic cells under hypoxia while leaving the normoxic cells intact.^{27,28}

Herein, we designed and fabricated light-activated hypoxia-responsive nanoparticles NPs-TPZ to codeliver TPZ and 5,10,5,20-tetrakis(4-aminophenyl)-porphine (TAPP) simultaneously through the synergy of π - π stacking, host-guest, and hydrophobic interactions for photodynamic chemotherapy (PDT-CT) (Scheme 1). After the nanoparticles NPs-TPZ

Received: December 15, 2024

Revised: April 24, 2025

Accepted: May 19, 2025

Published: May 30, 2025



Scheme 1. (A) Preparation of Nanoparticles NPs-TPZ and (B) Mechanism of NPs-TPZ for PDT-CT

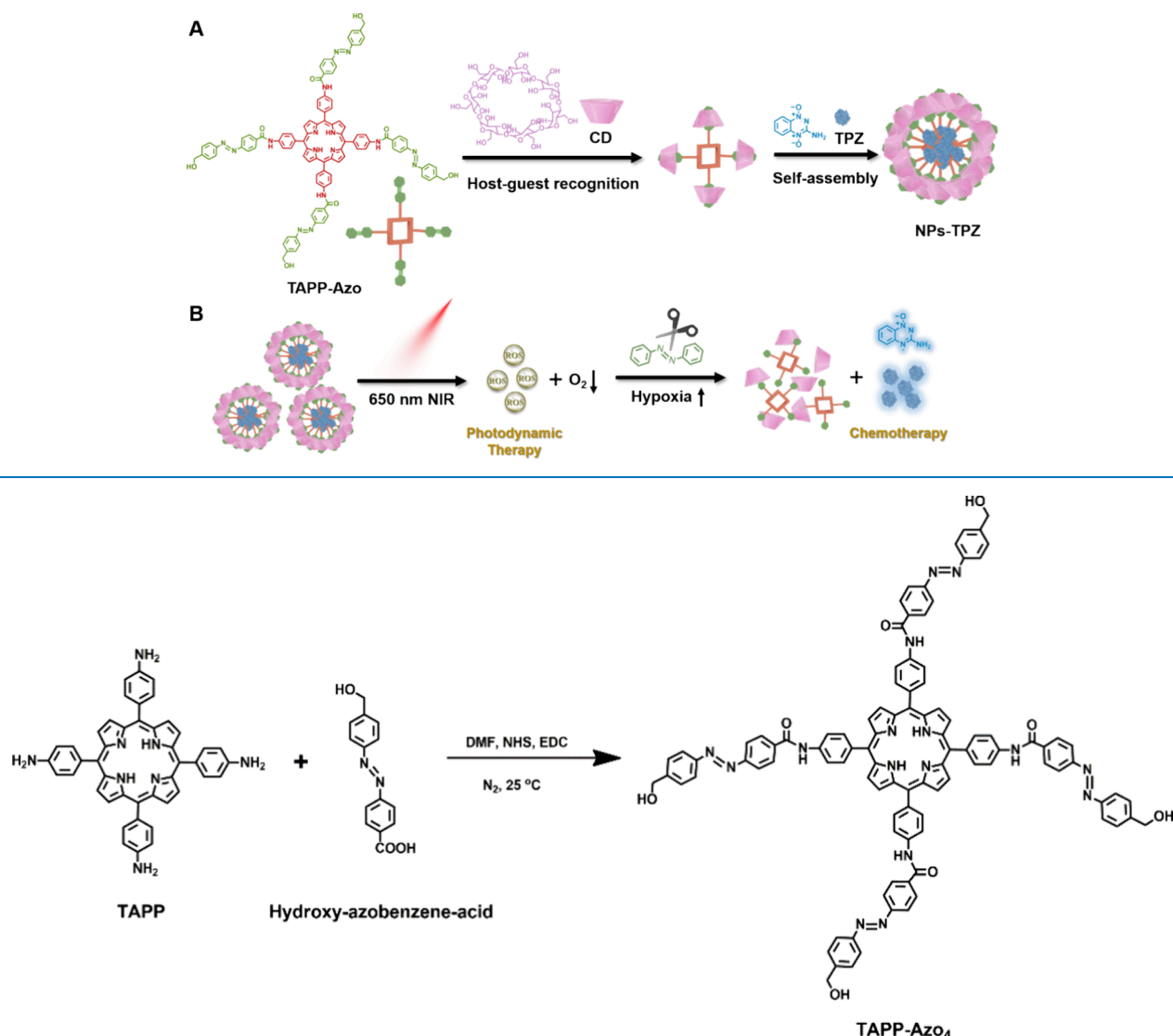


Figure 1. Synthetic route of TAPP-Azo.

were internalized by HeLa cells, in the hypoxic tumor microenvironment, NPs-TPZ rapidly disassembled and released a small quantity of TPZ due to the hypoxic-responsive cleavage of the azobenzene bond. Moreover, the TAPP component was capable of converting oxygen to produce singlet oxygen (¹O₂) upon near-infrared (NIR) irradiation, thereby specifically clearing cancer cells. Owing to the consumption of oxygen, the enhanced hypoxic environment by the induced PDT further facilitated the release of nontoxic TPZ. Under the exacerbated hypoxic microenvironment, TPZ was activated and converted into toxic benzotriazinyl (BTZ) radical to achieve therapeutic effects. In summary, the nanoparticles NPs-TPZ provide a new approach for inhibiting tumor growth with minimal side effects and synergistic PDT-CT under NIR.

2. MATERIALS AND METHODS

2.1. Reagents and Materials. TPZ, 1-(3-(dimethylamino)propyl)-3-ethylcarbodiimide hydrochloride (EDC), *N*-hydroxysuccinimide (NHS), and 5,10,5,20-tetrakis-(4-aminophenyl)-porphine (TAPP) were purchased from

Adamas (China). Hydroxy-azobenzene-acid was synthesized following the previous paper.¹⁸

2.2. Synthesis of TAPP-Azo. EDC (163.2 mg, 0.84 mmol) and NHS (98.4 mg, 0.83 mmol) were added to anhydrous DMF (20 mL) of hydroxy-azobenzene-acid (143.4 mg, 0.56 mmol) under N₂ conditions and stirred for 3 h. Next, an anhydrous DMF solution (15 mL) of TAPP (500 mg, 0.76 mmol) was added to the reaction solution and continued to react for 24 h. The removal of DMF was achieved through rotary evaporation, followed by purification of the residues using silica column chromatography to obtain TAPP-Azo.

2.3. Fabrication of Polymeric Nanoparticles NPs-TPZ. In general, TAPP-Azo (5.0 mg) and TPZ (5.0 mg) were dissolved in 1 mL of DMF and then stirred in the dark for 6 h. After that, a solution of CD (10 mg) was added to the original solution, and the mixture was vigorously stirred overnight. The resulting mixture was then placed into a dialysis tube (MWCO 1500 Da) and dialyzed against deionized water to get NPs-TPZ.

2.4. Detection of ¹O₂. The ABDA solution at a concentration of 0.05 mg/mL was mixed with 20 mL of PBS

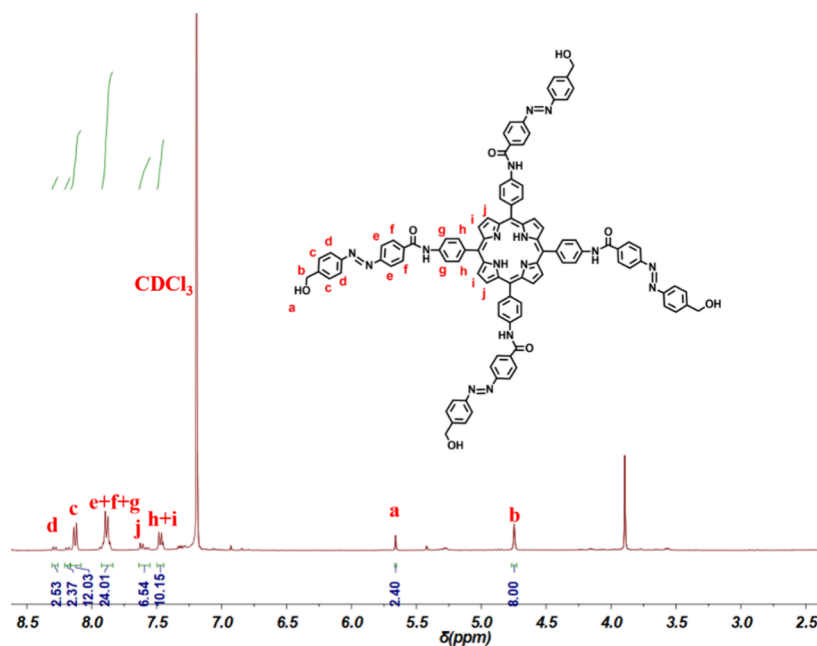


Figure 2. ^1H NMR spectra of TAPP-Azo (CDCl_3).

containing NPs-TPZ with a TAPP concentration of $40 \mu\text{g}/\text{mL}$. The mixed solution was then subjected to laser irradiation (650 nm , $0.5 \text{ W}/\text{cm}^2$, 5 min) for NIR-triggered $^1\text{O}_2$ release. Subsequently, the UV–vis spectroscopy analysis was conducted to measure the absorption intensity of ABDA.

2.5. In Vitro Drug Release. The PBS solution of $\text{Na}_2\text{S}_2\text{O}_4$ at a concentration of 3.2 mM was used to construct an in vitro hypoxic environment. The dialysis bag containing NPs-TPZ in PBS ($1 \text{ mg}/\text{mL}$) was immersed in a PBS solution of $\text{Na}_2\text{S}_2\text{O}_4$ at 37°C . The original dialysate was replaced with fresh dialysate at specific time points. For the irradiation groups, samples were exposed to NIR irradiation (650 nm , $1 \text{ W}/\text{cm}^2$, and 5 min) at predetermined times. The amount of released substance was measured using UV–vis spectroscopy.

2.6. In Vitro Cytotoxicity. HeLa cells were seeded in a 96-well plate and incubated for 12 h . After that, the medium was replaced with new DMEM containing NPs or NPs-TPZ at varying concentrations and incubated for another 6 h . For the groups subjected to irradiation, the cells were exposed to NIR irradiation (650 nm , $0.5 \text{ W}/\text{cm}^2$, 5 min) and then further incubated for 18 h . At last, cytotoxicity was assessed by the MTT method.

3. RESULTS AND DISCUSSION

The compound TAPP-Azo was prepared following the synthetic pathway outlined in Figure 1 and characterized by the relevant ^1H NMR and ^{13}C NMR spectra (Figures 2 and S1). As illustrated in Figure 2, all proton peaks corresponded to pure TAPP-Azo, suggesting successful preparation. Then, NPs-TPZ for codelivering TPZ and TAPP was fabricated referring to the dialysis method in previous reports.^{29–31} The CD aqueous solution is gradually dropped into the DMF solution of TAPP-Azo and TPZ under strong agitation to acquire NPs-TPZ. The blank NPs were established without TPZ as the control group. Both the UV–vis absorption spectra and fluorescence spectra of NPs-TPZ demonstrated the composition of the nanoparticles (Figure S2). The hydrodynamic diameter (D_h) of blank NPs was approximately 57.7

$\pm 3.9 \text{ nm}$ ($\text{PDI} = 0.3 \pm 0.06$) using dynamic light scattering (DLS) (Figure 3A). Meanwhile, the morphology of NPs was a

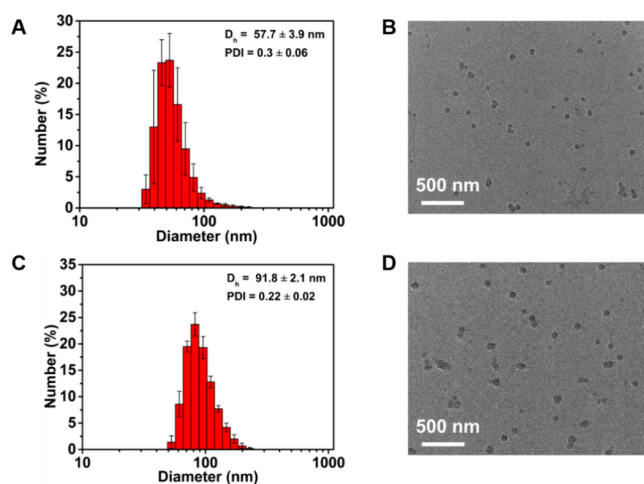


Figure 3. DLS data and TEM images of NPs (A, B) and NPs-TPZ (C, D).

spherical micelle based on the transmission electron microscopy (TEM) data (Figure 3B). After loading TPZ, nanoparticle NPs-TPZ displayed a slightly increased D_h with $91.8 \pm 2.1 \text{ nm}$ ($\text{PDI} = 0.22 \pm 0.02$) and a similar spherical micelle morphology (Figure 3C,D). This increased D_h demonstrated the successful encapsulation of TPZ and was suitable for transport to tumor tissue through the enhanced permeation and retention (EPR) effect.^{32–34}

To measure the NIR-induced $^1\text{O}_2$ generation, 9,10-anthracenediyl-bis(methylene) dimalonate (ABDA) was applied as an indicator of the ability of NPs-TPZ to generate $^1\text{O}_2$, which was directly related to the PDT efficiency. Regarding the fact that ABDA had the possibility of irreversibly reacting with $^1\text{O}_2$, the rapid reduction in ABDA absorbance suggests that NPs-TPZ can effectively produce $^1\text{O}_2$ under 650

nm NIR irradiation (0.5 W/cm^2 , 5 min) (Figure 4A).^{35,36} Therefore, the photosensitizer TAPP in nanoparticle NPs-TPZ can effectively generate $^1\text{O}_2$, supporting its suitability for PDT in hypoxic tumors.

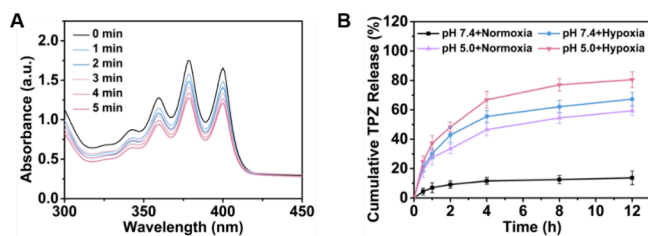


Figure 4. (A) Absorption spectra of ABDA under NIR irradiation (650 nm , 0.5 W/cm^2 , 5 min) by $^1\text{O}_2$ generated from NPs-TPZ. (B) Cumulative TPZ release profiles of NPs-TPZ with and without NIR laser irradiation. Data are expressed as the mean \pm SD ($n = 3$).

Thereafter, we monitored the characteristic absorption band of Azo bonds at 325 nm under a hypoxic environment to investigate the breaking of Azo bonds. As shown in Figure S3, the absorption peak at 325 nm decreased distinctly under hypoxia, while the absorption peak was almost unchanged under normoxia, indicating the hypoxia-responsive breakage of Azo in NPs-TPZ. The in vitro release of TPZ from NPs-TPZ was investigated under normoxic or hypoxic circumstances at various pH (Figure 4B). The release of TPZ reached 67.3 and 59.4% at pH 7.4 under hypoxia and at pH 5.0 under normoxia, respectively. In sharp contrast, under hypoxia conditions of pH 5.0, TPZ rose significantly to 80.5% after 12 h of hypoxia due to the synergistic effect of hypoxia/pH-responsive degradation of NPs-TPZ. This proves the weakening of host–guest interaction between CD and Azo and the hypoxia-induced fracture of Azo. Therefore, these results demonstrated that NPs-TPZ could be disassembled and further release activated TPZ for CT through the synergy of hypoxia and acid pH.

Then, the NIR-triggered $^1\text{O}_2$ generation was quantified in HeLa cells using a fluorescent probe (DCFH-DA), which could trap ROS through a rapid reaction with the anthracene moiety, subsequently resulting in the generation of green fluorescence. In the absence of NIR irradiation, negligible green fluorescence was observed in HeLa cells under both normoxia and hypoxia, indicating a high ROS concentration (Figure 5). By comparison, NPs-TPZ-treated HeLa cells plus NIR irradiation showed strong green fluorescence. Especially, the green fluorescence under normoxia was brighter than that

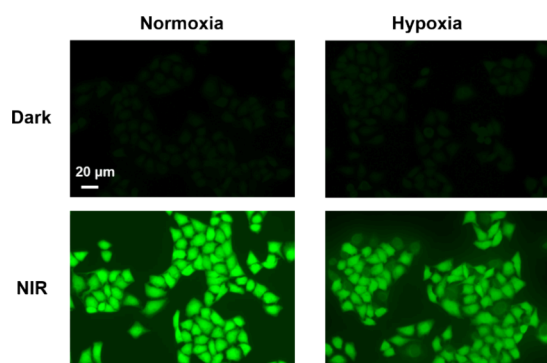


Figure 5. Confocal images of the generation of $^1\text{O}_2$ after different treatments by using a DCFH-DA probe.

under hypoxia, demonstrating that the efficacy of PDT was inhibited to a certain extent in a hypoxic environment. Furthermore, the flow cytometry analysis was used to investigate the intracellular light-triggered ROS generation, which showed the same result as that obtained by confocal laser scanning microscopy (CLSM) (Figure S5). Overall, both the NPs and NPs-TPZ showed a highly efficient ROS generation capacity under 650 nm irradiation.

Finally, the viability of HeLa cells incubated with NPs-TPZ under different conditions was evaluated by the MTT assay. After treatment for 48 h, the NPs-TPZ showed little dark cytotoxicity to HeLa cells and L929 cells under normoxic conditions without 650 nm irradiation (Figures 6A and S4),

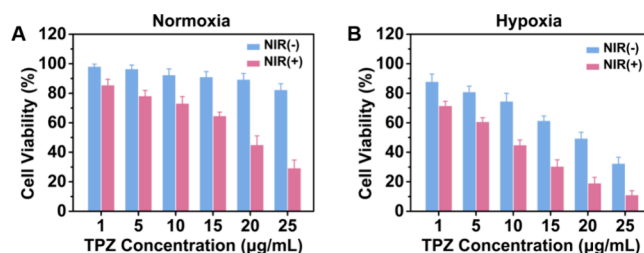


Figure 6. Relative cell viability of NPs-TPZ against HeLa cells under normoxia (A) or hypoxia (B) ($n = 6$; mean \pm SD).

confirming its superior biocompatibility. The NPs-TPZ + NIR group under normoxia exhibited considerable inhibition of HeLa cell proliferation due to the therapeutic effect of PDT-CT, while the NPs-TPZ under hypoxia without NIR irradiation also presented moderate cytotoxicity, contributing to the hypoxia-activated CT (Figure 6B). In sharp contrast, the NPs-TPZ + NIR group under hypoxia displayed the lowest cell viability. This result was determined by the generation of $^1\text{O}_2$ and PDT-induced hypoxia, which causes the hypoxia-responsive cleavage of Azo to release the drug TPZ and the following activation of TPZ.

4. CONCLUSIONS

In summary, we synthesized 5,10,5,20-tetrakis(4-aminophenyl)-porphine with four azobenzene groups to acquire hypoxia-responsive TAPP-Azo. Then, the hypoxia-responsive nanoparticles NPs-TPZ were further formed with CD and TAPP-Azo, which could passively accumulate at the tumor site through the EPR effect and achieve light-actuated PDT under 650 nm laser irradiation. During the process of photodynamic therapy, the hypoxia exacerbation owing to oxygen consumption caused the hypoxic-responsive cleavage of Azo, which accelerated the release and activation of TPZ. This study offers great insights into the development of hypoxia-activated cancer therapy with minimal side effects.

■ ASSOCIATED CONTENT

Supporting Information

The Supporting Information is available free of charge at <https://pubs.acs.org/doi/10.1021/acsomega.4c11283>.

^{13}C NMR spectra of TAPP-Azo ($\text{DMSO-}d_6$) (Figure S1); UV–vis absorption spectra and fluorescence spectra of NPs-TPZ at an excitation wavelength of 440 nm (Figure S2); azo degradation of NPs-TPZ under normoxia or hypoxia (Figure S3); and cytotoxicity of NPs-TPZ incubated with L929 cell lines under normoxic

conditions without 650 nm irradiation (Figure S4) (PDF)

AUTHOR INFORMATION

Corresponding Authors

Hongyang Xu – Department of Intensive Care Unit, The Affiliated Wuxi People's Hospital of Nanjing Medical University, Wuxi Medical Center, Nanjing Medical University, Wuxi People's Hospital, Wuxi 214023 Jiangsu, China; Email: xhy1912@aliyun.com

Yue Ding – School of Chemistry and Chemical Engineering, Nantong University, Nantong 226019, P. R. China; orcid.org/0000-0002-8857-4855; Email: yueding@ntu.edu.cn

Fengming Liang – Department of Intensive Care Unit, The Affiliated Wuxi People's Hospital of Nanjing Medical University, Wuxi Medical Center, Nanjing Medical University, Wuxi People's Hospital, Wuxi 214023 Jiangsu, China; Email: liangnanyi@sina.com

Authors

Dan Zhao – Department of Intensive Care Unit, The Affiliated Wuxi People's Hospital of Nanjing Medical University, Wuxi Medical Center, Nanjing Medical University, Wuxi People's Hospital, Wuxi 214023 Jiangsu, China

Shunliang Zheng – School of Chemistry and Chemical Engineering, Nantong University, Nantong 226019, P. R. China

Xinyi Zuo – School of Chemistry and Chemical Engineering, Nantong University, Nantong 226019, P. R. China

Complete contact information is available at: <https://pubs.acs.org/10.1021/acsomega.4c11283>

Notes

The authors declare no competing financial interest.

ACKNOWLEDGMENTS

This work was financially supported by the Nantong Science and Technology Project (MS2023040) and the Natural Science Foundation of Jiangsu Province (BK20240950).

REFERENCES

- (1) Chen, Y.; Xiang, H.; Zhuang, S.; Shen, Y.; Chen, Y.; Zhang, J. Oxygen-independent photocleavage of radical nanogenerator for near-IR-gated and H₂O-mediated free-radical nanotherapy. *Adv. Mater.* **2021**, *33*, No. e2100129.
- (2) Shen, D.; Ding, S.; Lu, Q.; Chen, Z.; Chen, L.; Lv, J.; Gao, J.; Yuan, Z. Nitroreductase-responsive fluorescent “off-on” photosensitizer for hypoxic tumor imaging and dual-modal therapy. *ACS Omega* **2024**, *9*, 30685–30697.
- (3) Akdogan, C. Z. S.; Çetin, E. A.; Onur, M. A.; Önel, S.; Tuncel, A. In vitro synergistic photodynamic, photothermal, chemodynamic, and starvation therapy performance of chlorin e6 immobilized, polydopamine-coated hollow, porous ceria-based, hypoxia-tolerant nanozymes carrying a cascade system. *ACS Appl. Bio Mater.* **2024**, *7*, 2781–2793.
- (4) Ding, Y.; Wang, C.; Ma, Y.; Zhu, L.; Lu, B.; Wang, Y.; Wang, J.; Chen, T.; Dong, C. M.; Yao, Y. pH/ROS dual-responsive supramolecular polypeptide prodrug nanomedicine based on host-guest recognition for cancer therapy. *Acta Biomater.* **2022**, *143*, 381–391.
- (5) Zhu, J.; Wang, W.; Wang, X.; Zhong, L.; Song, X.; Wang, W.; Zhao, Y.; Dong, X. Multishell nanoparticles with “linkage mechanism” for thermal responsive photodynamic and gas synergistic therapy. *Adv. Healthcare Mater.* **2021**, *10*, No. 2002038.
- (6) Liu, X.; Wang, H.; Li, Z.; Li, J.; He, S.; Hu, C.; Song, Y.; Gao, H.; Qin, Y. Transformable self-delivered supramolecular nanomaterials combined with anti-PD-1 antibodies alleviate tumor immunosuppression to treat breast cancer with bone metastasis. *J. Nanobiotechnol.* **2024**, *22* (1), 566.
- (7) Qian, C.; Yu, J.; Chen, Y.; Hu, Q.; Xiao, X.; Sun, W.; Wang, C.; Feng, P.; Shen, Q. D.; Gu, Z. Light-activated hypoxia-responsive nanocarriers for enhanced anticancer therapy. *Adv. Mater.* **2016**, *28* (17), 3313–3320.
- (8) Ding, Y.; Yu, W.; Wang, J.; Ma, Y.; Wang, C.; Wang, Y.; Lu, B.; Yao, Y. Intelligent supramolecular nanoprodruge based on anionic water-soluble [2]biphenyl-extended-pillar[6]arenes for combination therapy. *ACS Macro Lett.* **2022**, *11*, 830–834.
- (9) Wang, H.; Wu, H.; Yi, Y.; Xue, K.-F.; Xu, J.-F.; Wang, H.; Zhao, Y.; Zhang, X. Self-motivated supramolecular combination chemotherapy for overcoming drug resistance based on acid-activated competition of host-guest interactions. *CCS Chem.* **2021**, *3*, 1413–1425.
- (10) Mousazadeh, H.; Bonabi, E.; Zarghami, N. Stimulus-responsive drug/gene delivery system based on polyethylenimine cyclodextrin nanoparticles for potential cancer therapy. *Carbohydr. Polym.* **2022**, *276*, No. 118747.
- (11) Yan, M.; Wu, S.; Wang, Y.; Liang, M.; Wang, M.; Hu, W.; Yu, G.; Mao, Z.; Huang, F.; Zhou, J. Recent progress of supramolecular chemotherapy based on host-guest interactions. *Adv. Mater.* **2024**, *36* (21), No. e2304249.
- (12) Li, X.; Shen, M.; Yang, J.; Liu, L.; Yang, Y. W. Pillararene-based stimuli-responsive supramolecular delivery systems for cancer therapy. *Adv. Mater.* **2024**, *36* (16), No. e2313317.
- (13) Liu, C.; Bu, H.; Duan, X.; Li, H.; Bai, Y. Host-guest interaction-based supramolecular self-assemblies for H₂O₂ upregulation augmented chemiluminescence resonance energy transfer-induced cancer therapy. *ACS Appl. Mater. Interfaces* **2023**, *15* (32), 38264–38272.
- (14) He, H.; Du, L.; Xue, H.; Wu, J.; Shuai, X. Programmable therapeutic nanoscale covalent organic framework for photodynamic therapy and hypoxia-activated cascade chemotherapy. *Acta Biomater.* **2022**, *149*, 297–306.
- (15) Xu, Z.; Zhang, X.; Shan, Q.; Zhu, W.; Jiang, S.; Li, R.; Wu, X.; Huo, M.; Ying, B.; Chen, C.; Chen, X.; Zhang, K.; Chen, W.; Chen, J. Fluorocarbon-functionalized polymerization-induced self-assembly nanoparticles alleviate hypoxia to enhance sonodynamic cancer therapy. *Adv. Healthcare Mater.* **2024**, *14*, No. e2403251.
- (16) Wang, M.; Zhang, Z.; Li, Q.; Liu, R.; Li, J.; Wang, X. Multifunctional nanoplatform with near-infrared triggered nitric-oxide release for enhanced tumor ferroptosis. *J. Nanobiotechnol.* **2024**, *22* (1), 656.
- (17) Zhao, D.; Zhang, Y.; Yan, Z.; Ding, Y.; Liang, F. Hypoxia-responsive polymeric nanoprodruge for combo photodynamic and chemotherapy. *ACS Omega* **2024**, *9*, 1821–1826.
- (18) Ding, Y.; Yu, W.; Shen, R.; Zheng, X.; Zheng, H.; Yao, Y.; Zhang, Y.; Du, C.; Yi, H. Hypoxia-responsive tetrameric supramolecular polypeptide nanoprodruge for combination therapy. *Adv. Healthcare Mater.* **2023**, *13*, No. 2303308.
- (19) Zhao, Y.-Y.; Zhang, X.; Xu, Y.; Chen, Z.; Hwang, B.; Kim, H.; Liu, H.; Li, X.; Yoon, J. A renal clearable nano-assembly with forster resonance energy transfer amplified superoxide radical and heat generation to overcome hypoxia resistance in phototherapeutics. *Angew. Chem., Int. Ed.* **2024**, *63*, No. e202411514.
- (20) Li, H.; Zhang, X.; Chen, S.; Cao, C.; Zhang, X.; Li, X.; Xing, S.; Jia, S.; Li, J.; Wang, S. Hypoxia exacerbation-triggered doxorubicin prodruge activation for sequential photodynamic/chemotherapy. *ACS Mater.* **2024**, *6* (7), 2599–2608.
- (21) Li, X.; Jeon, Y.-H.; Kwon, N.; Park, J.-G.; Guo, T.; Kim, H.-R.; Huang, J.-D.; Lee, D.-S.; Yoon, J. In vivo-assembled phthalocyanine/albumin supramolecular complexes combined with a hypoxia-activated prodruge for enhanced photodynamic immunotherapy of cancer. *Biomaterials* **2021**, *266*, No. 120430.
- (22) Lu, J.; Yu, J.; Xie, W.; Gao, X.; Guo, Z.; Jin, Z.; Li, Y.; Fahad, A.; Pambe, N. U.; Che, S.; Wei, Y.; Zhao, L. Physical dissolution

combined with photodynamic depletion: a two-pronged nano-approach for deoxygenation-driven and hypoxia-activated prodrug therapy. *ACS Appl. Bio Mater.* **2023**, *6*, 3902–3911.

(23) Hao, Y.; Gao, Y.; Fan, Y.; Zhang, C.; Zhan, M.; Cao, X.; Shi, X.; Guo, R. A tumor microenvironment-responsive poly(amidoamine) dendrimer nanoplatform for hypoxia-responsive chemo/chemodynamic therapy. *J. Nanobiotechnol.* **2022**, *20* (1), 43.

(24) Hou, X.; Chang, Y. X.; Yue, Y. X.; Wang, Z. H.; Ding, F.; Li, Z. H.; Li, H. B.; Xu, Y.; Kong, X.; Huang, F.; Guo, D. S.; Liu, J. Supramolecular radiosensitizer based on hypoxia-responsive macrocycle. *Adv. Sci.* **2022**, *9* (6), No. 2104349.

(25) Deng, F.; Yan, M.; Liu, Y.; Wang, R.; He, H.; Chen, A.; Wang, J.; Xu, L.; Yang, B.; Cheng, H.; Li, S. Self-delivery of metal-coordinated mitochondria protonophore uncoupler for O₂-exhausting enhanced bioreductive therapy. *Biomaterials* **2022**, *286*, No. 121576.

(26) Pucelik, B.; Sulek, A.; Barzowska, A.; Dabrowski, J. M. Recent advances in strategies for overcoming hypoxia in photodynamic therapy of cancer. *Cancer Lett.* **2020**, *492*, 116–135.

(27) Dong, X.; Brahma, R. K.; Fang, C.; Yao, S. Q. Stimulus-responsive self-assembled prodrugs in cancer therapy. *Chem. Sci.* **2022**, *13* (15), 4239–4269.

(28) Du, C.; Wang, C.; Jiang, S. H.; Zheng, X.; Li, Z.; Yao, Y.; Ding, Y.; Chen, T.; Yi, H. pH/GSH dual-responsive supramolecular nanomedicine for hypoxia-activated combination therapy. *Biomater. Sci.* **2023**, *11* (16), 5674–5679.

(29) Pei, P.; Sun, C.; Tao, W.; Li, J.; Yang, X.; Wang, J. ROS-sensitive thioketal-linked polyphosphoester-doxorubicin conjugate for precise phototriggered locoregional chemotherapy. *Biomaterials* **2019**, *188*, 74–82.

(30) Tan, G.; Wang, Y.; He, Y.; Miao, G.; Li, Y.; Wang, X. Bioinspired poly(cation- π) micelles drug delivery platform for improving chemotherapy efficacy. *J. Controlled Release* **2022**, *349*, 486–501.

(31) Ling, T.; Huang, X.; Xie, Y.; Zheng, L.; Ding, Y.; Du, C.; Chen, J. A dendritic drug-drug conjugate self-assembled hypoxia-responsive supramolecular nanoparticle for combination therapy. *J. Mater. Chem. B* **2025**, *13*, 1961–1968.

(32) Ding, H.; Tan, P.; Fu, S.; Tian, X.; Zhang, H.; Ma, X.; Gu, Z.; Luo, K. Preparation and application of pH-responsive drug delivery systems. *J. Controlled Release* **2022**, *348*, 206–238.

(33) Hu, D.; Pan, M.; Yang, Y.; Sun, A.; Chen, Y.; Yuan, L.; Huang, K.; Qu, Y.; He, C.; Wei, Q.; Qian, Z. Trimodal sono/photoinduced focal therapy for localized prostate cancer: single-drug-based nano-sensitizer under dual-activation. *Adv. Funct. Mater.* **2021**, *31*, No. 2104473.

(34) Qian, Y.; Chen, W.; Wang, M.; Xie, Y.; Qiao, L.; Sun, Q.; Gao, M.; Li, C. Tumor microenvironment-specific driven nanoagents for synergistic mitochondria damage-related immunogenic cell death and alleviated immunosuppression. *Small Methods* **2024**, *8* (7), No. e2301231.

(35) Tang, X.; Chen, L.; Wang, Y.; Chen, P.; Li, L. S.; Yang, X.; Zhao, M. X. Multimodal phototherapy agents target lipid droplets for near-infrared imaging-guided type I photodynamic/photothermal therapy. *Acta Biomater.* **2024**, *180*, 394–406.

(36) Fang, B.; Bai, H.; Zhang, J.; Wang, L.; Li, P.; Ge, Y.; Yang, H.; Wang, H.; Peng, B.; Hu, W.; Ma, H.; Chen, X.; Fu, L.; Li, L. Albumins constraining the conformation of mitochondria-targeted photosensitizers for tumor-specific photodynamic therapy. *Biomaterials* **2025**, *315*, No. 122914.